Computational and Structural Biotechnology Journal 19 (2021) 4435–4446

COMPUTATIONAL AND STRUCTURAL BIOTECHNOLOGY JOURNAL

journal homepage: www.elsevier.com/locate/csbj

Revealing biomarkers associated with PARP inhibitors based on genetic interactions in cancer genome

Qi Dong [a,1], Mingyue Liu [a,1], Bo Chen [a,1], Zhangxiang Zhao [a], Tingting Chen [a], Chengyu Wang [a], Shuping Zhuang [a], Yawei Li [a], Yuquan Wang [a], Liqiang Ai [a], Yaoyao Liu [a], Haihai Liang [b], Lishuang Qi [a], Yunyan Gu [a,*]

[a] Department of Systems Biology, College of Bioinformatics Science and Technology, Harbin Medical University, Harbin, China
[b] Department of Pharmacology, College of Pharmacy, Harbin Medical University, Harbin, China

ARTICLE INFO

Article history:
Received 28 January 2021
Received in revised form 28 July 2021
Accepted 6 August 2021
Available online 10 August 2021

Keywords:
PARP inhibitors
Genetic interactions
Mutation
Resistant biomarkers
Sensitive biomarkers

ABSTRACT

Poly (ADPribose) polymerase inhibitors (PARPis) are clinically approved drugs designed according to the concept of synthetic lethality (SL) interaction. It is crucial to expand the scale of patients who can benefit from PARPis, and overcome drug resistance associated with it. Genetic interactions (GIs) include SL and synthetic viability (SV) that participate in drug response in cancer cells. Based on the hypothesis that mutated genes with SL or SV interactions with PARP1/2/3 are potential sensitive or resistant PARPis biomarkers, respectively, we developed a novel computational method to identify them. We analyzed fitness variation of cell lines to identify PARP1/2/3-related GIs according to CRISPR/Cas9 and RNA interference functional screens. Potential resistant/sensitive mutated genes were identified using pharmacogenomic datasets. We identified 41 candidate resistant and 130 candidate sensitive PARPi-response related genes, and observed that *EGFR* with gain-of-function mutation induced PARPi resistance, and predicted a combination therapy with PARP inhibitor (veliparib) and EGFR inhibitor (erlotinib) for lung cancer. We also revealed that a resistant gene set (*TNN*, *PLEC*, and *TRIP12*) in lower grade glioma and a sensitive gene set (*BRCA2*, *TOP3A*, and *ASCC3*) in ovarian cancer, which were associated with prognosis. Thus, cancer genome-derived GIs provide new insights for identifying PARPi biomarkers and a new avenue for precision therapeutics.

1. Background

Poly (ADP-ribose) polymerases (PARPs) are DNA repair enzymes that play roles in DNA damage repair and replication fork protection. In cancer therapy, PARP inhibitors (PARPis) target *PARP* genes by reducing DNA repair function and increasing replication fork errors in cancer cells [1]. Currently, four PARPis (olaparib, rucaparib, niraparib, and talazoparib) have been approved by the U.S. Food and Drug Administration. Additionally, PARPis have been included in the clinical guidelines for treatment of ovarian, breast, pancreatic, and prostate cancers, and clinical trials of PARPis in other cancers are under way.

PARPis are associated with resistance in clinical therapeutics. A possible mechanism of PARPi resistance includes restoration of homologous recombination (HR) repair ability due to secondary mutations in BRCA1/2, and depletion of HR compensatory repair pathways such as the non-homologous end joining pathway [2,3]. Patients with *BRCA1/2* mutations are sensitive to PARPis, where PARPis lead to cancer cell death by utilizing a synthetic lethality (SL) interaction with *BRCA1/2* deficiency. However, it is necessary to identify effective biomarkers to predict the response to PARPis in patients without BRCA1/2 mutations as well [4]. Thus, it is important to identify genomic biomarkers that overcome PARPi resistance and expand its application to promote precision medicine.

* Corresponding author at: Department of Systems Biology, College of Bioinformatics Science and Technology, Harbin Medical University, Harbin 150086, China.
E-mail addresses: dongqi0925@163.com (Q. Dong), liumingyue_1995@163.com (M. Liu), chenccc50@163.com (B. Chen), zjzhaozhangxiang@126.com (Z. Zhao), ttchen_0714@163.com (T. Chen), wangchengyutt@126.com (C. Wang), zsp102030@126.com (S. Zhuang), yaweili93@163.com (Y. Li), jjboy_8114222@163.com (Y. Wang), hyd2015alq@163.com (L. Ai), better_eleven_six@163.com (Y. Liu), lianghaihai@ems.hrbmu.edu.cn (H. Liang), qilishuang7@ems.hrbmu.edu.cn (L. Qi), guyunyan@ems.hrbmu.edu.cn (Y. Gu).

[1] Contributed equally to this work.

https://doi.org/10.1016/j.csbj.2021.08.007

SL and synthetic viability (SV) interactions are known as genetic interactions (GIs). GIs refer to the effect of simultaneous changes in two genes that is different from the expected additive effect of an individual change [5]. SL interaction is a phenomenon when two gene defects that cause cell death or significant impairment of fitness, emerge simultaneously. SL interactions contribute to the identification of new drug targets or drug sensitivity biomarkers [6]. Meanwhile, SV interaction refers to the combination of gene effects that rescue the lethal effects of single gene alterations. Our previous work has demonstrated that SV interactions in the cancer genome could induce drug resistance [7,8]. Our study aimed to detect PARPi response biomarkers using the GI network in cancer cells based on the hypothesis that genes with SL interactions with PARP1/2/3 may be potential sensitive biomarkers for PARPis, and genes with SV interactions with PARP1/2/3 may induce resistance to PARPis. However, the GI network for each cancer type is unavailable. Recent functional genomic technologies such as CRISPR/Cas9 assays and RNA interference (RNAi) have aided in detection of essential genes by gene knockdown and knockout, and have provided innovative tools to screen for cancer GIs [9]. For instance, CRISPR-based genetic screens have identified SL interactions and molecular functions of genes in acute myeloid leukemia cell lines [10]. Horn et al. have annotated metazoan genes based on GI profiles that were integrated by an RNAi-based experimental approach [11]. However, most studies focused on SL interactions and have ignored SV interactions as well as prediction values for determining drug response.

Thus, in this study, we proposed a novel computational method to identify candidate responsive resistant and sensitive biomarkers for PARPis by utilizing CRISPR/Cas9 and RNAi screens, and pan-cancer pharmacogenomic datasets.

2. Results

2.1. Identification of gene mutations as candidate biomarkers for PARPis

We used CRISPR/Cas9 and RNAi screens to identify PARP1/2/3-related GIs (Fig. 1A). If PARP1/2/3 was knocked down and gene A mutations caused a significant selective enhancement (or reduction) in cancer cell viability, then gene A mutations may have an SV (or SL) relationship with PARP1/2/3 inhibition. We identified mutated genes that significantly affected PARPi response (IC50 or area under the curve [AUC]) in specific cancer cell types (Fig. 1A; $P < 0.01$; one-sided Wilcoxon rank-sum test). Mutated genes, have SL interactions with PARP1/2/3 knockdown, were associated with PARPi sensitivity in cancer cells and predicted as candidate sensitive biomarkers of PARPis. Whereas, mutated genes that had an SV effect with PARP1/2/3 knockdown, and were associated with PARPi resistance in cancer cells, were predicted as resistant candidate biomarkers of PARPis (Fig. 1A; $P < 0.01$; one-sided Wilcoxon rank-sum test). In total, 41 resistant and 130 sensitive genes were identified as candidate biomarkers for PARPis (Fig. 2; Table S1).

Patients with *BRCA1/2* mutations are sensitive to PARPis in cancer cells. Our results showed that cancer cells with *BRCA2* mutations were sensitive to olaparib and niraparib in large intestine tissues (Fig. 3A, B; $P < 0.01$; one-sided Wilcoxon rank-sum test). In the Achilles shRNA dataset, after *PARP1* knockdown, large intestine cancer cells with *BRCA2* mutation showed poorer proliferation than cancer cells with wild type *BRCA2* (Fig. 3C; $P < 0.01$; one-sided Wilcoxon rank-sum test). Besides, according to olaparib response data in Genomics of Drug Sensitivity in Cancer (GDSC) and *PARP2* knockdown data, mutation of *BRCA1* was confirmed as a sensitive biomarker for PARPis (Fig. S1; $P < 0.05$; one-sided Wilcoxon rank-sum test). Moreover, mutations in some cancer genes, such as *RB1* (Fig. 3D-I; $P < 0.01$; one-sided Wilcoxon rank-sum test) and *MACF1* (Fig. S2A-F; $P < 0.01$; one-sided Wilcoxon rank-sum test), were predicted as candidate sensitive biomarkers for PARPis, and *RB1* and *TOP3A* mutations were predicted as candidate sensitive biomarkers for PARPis based on both AUC and IC50 values (Fig. 3D-P; $P < 0.01$; one-sided Wilcoxon rank-sum test). In GDSC database, *TTN* and *TRIP12* mutations were predicted as resistant biomarkers for PARPis based on both AUC and IC50 values (Fig. 3-Q-V; $P < 0.01$; one-sided Wilcoxon rank-sum test). Importantly, *RB1* and *NRDC* mutations were predicted as candidate sensitive biomarkers in both the GDSC database and Cancer Therapeutics Response Portal (CTRP; Fig. 3D-I for *RB1*; Fig. S2G-S for *NRDC*; $P < 0.01$; one-sided Wilcoxon rank-sum test).

The triple-negative breast cancer patients who treated with veliparib plus DNA-damaging agents (carboplatin and paclitaxel) were used to validate proposed biomarkers [12]. Mutations of *PPP1R12B* was predicted as a sensitive biomarker of PARPi in breast cancer (BRCA). BRCA with *PPP1R12B* mutations showed lower expression than BRCA with wild type *PPP1R12B* in The Cancer Genome Atlas (TCGA) (Fig. S3A; $P = 9.0E-02$; one-sided Wilcoxon rank-sum test). The expression of *PPP1R12B* in pathological complete response (pCR) patients were significantly lower than those in residual disease (RD) patients (Fig. S3B; $P = 5.0E-02$; one-sided Wilcoxon rank-sum test).

In addition, we obtained drug response data (IC50 and AUC) of four PARPis (PARP_0108, PARP_9482, PARP_9495 and TANK_1366) from GDSC for further validation. IC50 and AUC values in cell lines with mutations of resistant genes (e.g. *FREM1* and *PCDH12*) were higher than cell lines with wild type resistant genes in at least three PARPis (Fig. S4A, B; $P < 0.05$; one-sided Wilcoxon rank-sum test). IC50 and AUC values in cell lines with mutations of some sensitive genes (e.g. *MACF1*, *TOP3A,* and *NOTCH1*) were lower than cell lines with wild type resistant genes in three PARPis (Fig. S4C-E; $P < 0.05$; one-sided Wilcoxon rank-sum test).

2.2. Disrupting HR to mediate response to PARPis in cancer cells

PARP inhibition causes SL in cancers with defects in HR. However, HR restoration leads to resistance to PARPis even in cancers with *BRCA1/2* mutations or hypermethylation [13]. Thus, we investigated whether the genomic biomarkers predicted by GI could disrupt HR to mediate the response of PARPis in cancer cells (Fig. 1B). We found that HR proteins were significantly differentially expressed in cancer samples with mutations of biomarker genes than in cancer samples with wild type biomarker genes (Fig. 4; $P < 0.05$; one-sided Wilcoxon rank-sum test). According to HR protein expression analysis, resistant genes affected the expression of HR proteins such as RAD51 and BRCA2 (Fig. 4A, B). Expression of RAD50 was significantly downregulated by 44.0% (62/141) sensitive genes in TCGA data and 44.3% (43/97) sensitive genes in Cancer Cell Line Encyclopedia (CCLE) data (Fig. 4C, D). *RAD50* deletion is a candidate marker of response to PARPis in BRCA wild type ovarian cancer [14]. Furthermore, expression of ATM protein was significantly downregulated by 37.6% (53/141) sensitive genes in TCGA data and 42.3% (41/97) sensitive genes in CCLE data (Fig. 4C, D). Further, *ATM* mutant cell line significantly reduces cancer load and increases survival of animals after olaparib treatment in vivo, and *ATM* depletion sensitizes breast cancer cells to PARP inhibition [15,16].

Homologous recombination deficiency (HRD) genomic scarring was scored by sum of telomeric allelic imbalance (TAI) score, the large-scale state transitions (LST) score and the loss of heterozygosity (LOH) score [17]. We investigated the effect of candidate biomarker mutation on HRD by testing the HRD score between groups of mutated and wild type candidate biomarkers. HRD score was significantly lower in the mutation group than wild type of

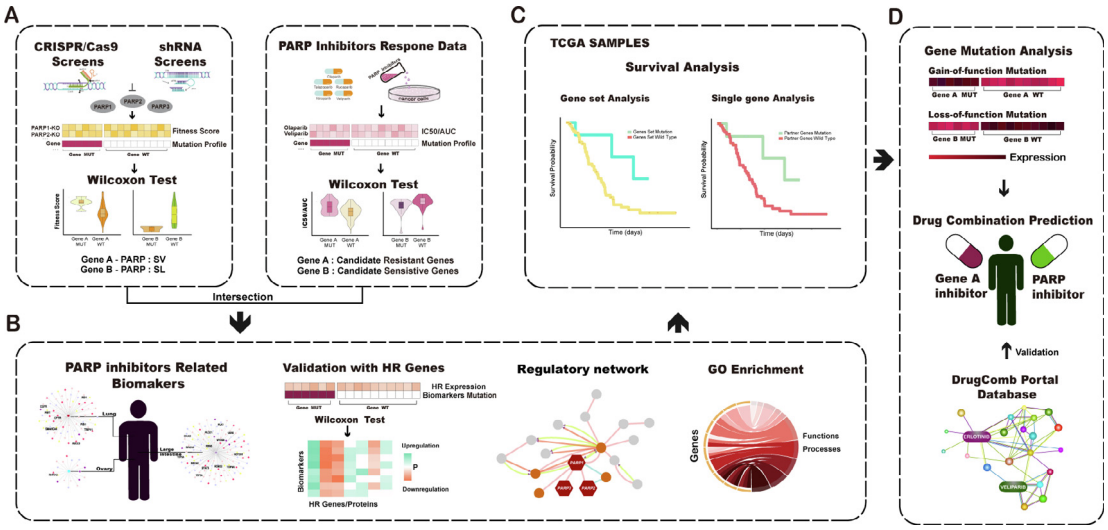

Fig. 1. Workflow of the study. (A) Identification of potential biomarkers for PARP inhibitors (PARPis) using cancer genome data. (B) Mechanism analysis for biomarkers. (C) Verification of biomarkers for PARPis in The Cancer Genome Atlas (TCGA). (D) Prediction of drug combination with PARPis.

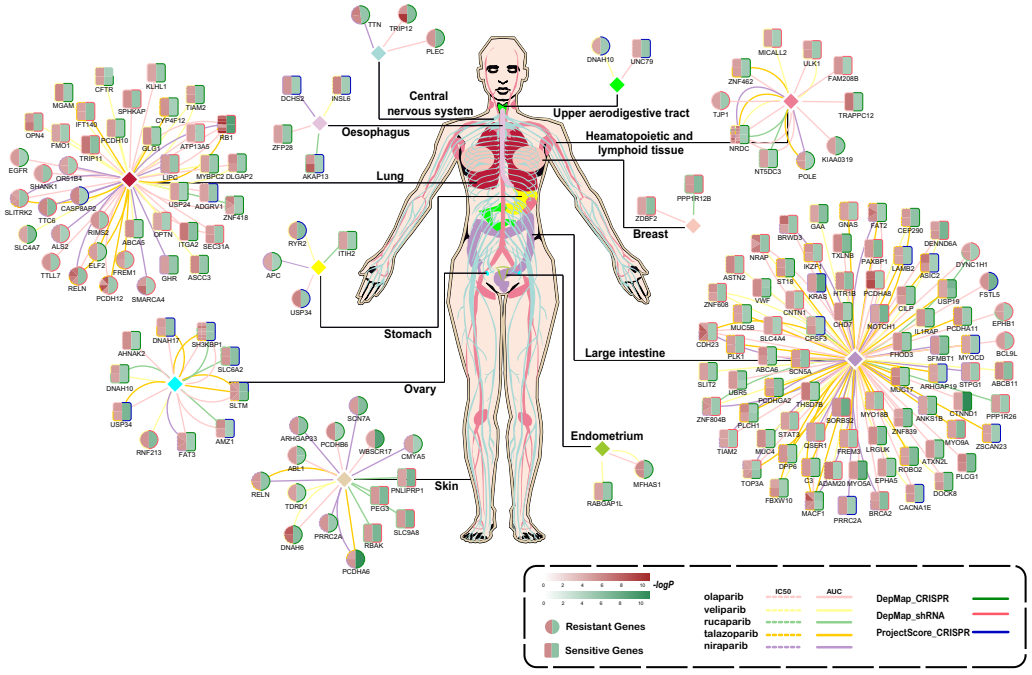

Fig. 2. Candidate genomic biomarkers for PARP inhibitors (PARPis) in cancer. Each diamond-marked module shows mutated genes as biomarkers for PARPis predicted in 11 cancer tissues. Circle nodes indicate PARPi resistance-related mutated genes and square nodes indicate PARPi sensitivity-related mutated genes. Node color corresponds to -*logP*, where *P* values were calculated using Wilcoxon rank-sum test. The red part indicates the significance that was tested from pharmacogenomic datasets of PARPis, and the green part depicts the significance that was tested using CRISPR/Cas9 and RNA interference functional screens. The border color of the nodes in red indicates different drugs: pink is olaparib, yellow is veliparib, green is rucaparib, orange is talazoparib, and purple is niraparib. Dashed line of the node border represents the *P* value from IC50, and the solid line indicates the *P* value from area under the curve (AUC). Border color of the node in the green part shows the significance detected in DepMap_CRISPR (green), DepMap_shRNA (red), and ProjectScore_CRISPR (blue). Edge colors denote the five PARPis. (For interpretation of the references to color in this figure legend, the reader is referred to the web version of this article.)

proposed resistant genes in TCGA, such as *DYNC1H1*, *BCL9L,* and *MFHAS1* (Fig. S5A-C; *P* = 3.1E-09 for *DYNC1H1*, *P* = 4.6E-05 for *BCL9L*, *P* = 7.1E-04 for *MFHAS1*; one-sided Wilcoxon rank-sum test). HRD score was significantly higher in the mutation group than wild type of proposed sensitive genes, such as *PCDH10*, *GHR,* and *TRIP11* in LUAD (Fig. S5D-F; *P* = 1.2E-05 for *PCDH10*, *P* = 1.5E-05 for *GHR*, *P* = 4.9E-04 for *TRIP11*; one-sided Wilcoxon rank-sum test). The above results confirmed that mutated genes that were predicted as candidate biomarkers might affect the therapeutic effect of PARPis by disrupting the HR mechanism.

2.3. PARPi response proposed biomarkers have functional interactions with PARP1/2/3

We suspected that PARPi-related resistant or sensitive genes might interact with PARP1/2/3 to affect the pharmacodynamic effect of PARPis through functional regulation. Thus, we constructed protein–protein interaction (PPI) networks of proposed resistant or sensitive genes and PARP1/2/3. Most drug response genes directly or indirectly interacted with PARP1/2/3, especially cancer-related genes (e.g., *EGFR*, *ABL1*, and *RB1*) and DNA damage

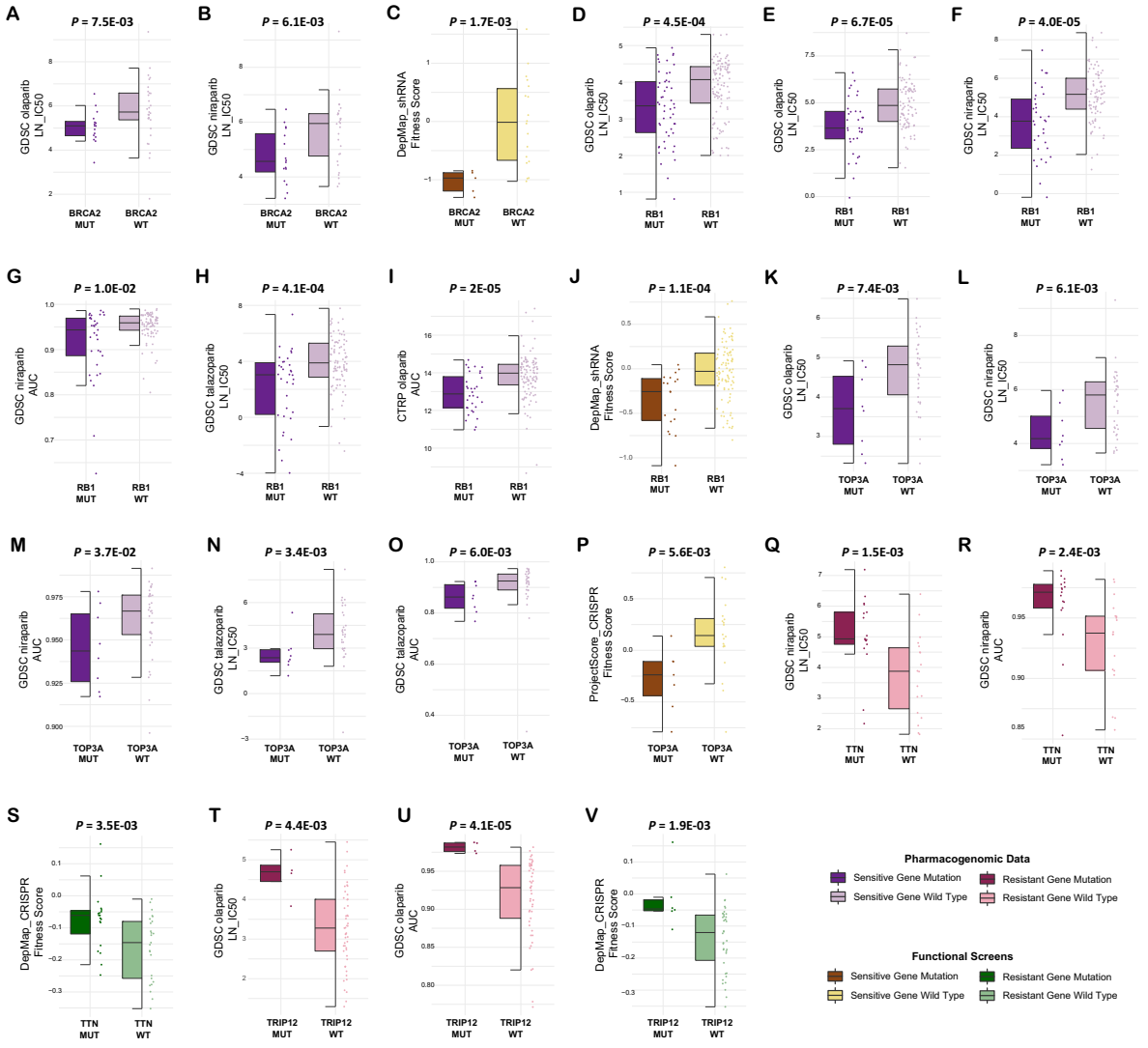

Fig. 3. Candidate biomarkers for PARP inhibitors (PARPis) in cancer. (A-C) Large intestine cell lines with *BRCA2* mutation are sensitive to PARPis in Genomics of Drug Sensitivity in Cancer (GDSC) data, and have worse viability when *PARP1* is knocked down in DepMap_shRNA data. (D-J) Lung cell lines with *RB1* mutation are sensitive to PARPis in GDSC and Cancer Therapeutics Response Portal (CTRP), and have worse viability when *PARP3* is knocked down in DepMap_shRNA data. (K-P) Large intestine cell lines with *TOP3A* mutation are sensitive to PARPis in GDSC, and have worse viability when *PARP2* is knocked down in ProjectScore_CRISPR data. (Q-S) Central nervous system cell lines with *TTN* mutation are resistant to PARPis in GDSC, and have better viability when *PARP3* is knocked down in DepMap_CRISPR data. (T-V) Central nervous system cell lines with *TRIP12* mutation are resistant to PARPis in GDSC, and have better viability when *PARP3* is knocked down in DepMap_CRISPR data. Biomarkers identified in GDSC1 or GDSC2 are labeled as "GDSC".

repair (DDR) genes (e.g., *BRCA2*, *ASCC3*, *TOP3A*, and *SMARCA4*). *EGFR* was a hub gene in the PARPi-resistant PPI network, and controlled the state change of *PARP1*. Candidate resistant *TJP1* and *TTN* genes, neighbors of *EGFR*, indirectly interacted with *PARP1* (Fig. 5A). *TJP1* plays a role in regulating cell adhesion and matrix remodeling, and loss of *TJP1* causes MCF10A cells to become resistant to PARPis, including olaparib, veliparib, talazoparib, and rucaparib [18,19]. Fig. 5B shows the proposed sensitive genes of PARPis and PARP1/2/3 interaction network, within which the SL effects observed between hub genes (*RB1*, *BRCA2*, *KRAS*, etc.) and PARP1/2/3 have been reported in previous studies. For instance, mutations in *KRAS* have SL interactions with PARP1/2 knockout in colon adenocarcinoma [20]. Large intestine cancer cell lines with *KRAS* mutations were sensitive to PARPis in GDSC (AUC; P = 5.8E-03 for niraparib; one-side Wilcoxon rank-sum test) and had SL interactions with *PARP3* in ProjectScore_CRISPR data (P = 2.5E-04; one-sided Wilcoxon rank-sum test). Moreover, we found that *RB1* mutations could mediate the sensitivity to PARPis in lung cancer cell lines (Fig. 3D-J), which is consistent with previous findings that *RB1* has SL interactions with PARP1 in multiple cancers, including lung adenocarcinoma [9]. Large intestine cell lines with cancer gene *STAT3* mutation were sensitive to PARPis in GDSC (IC50; P = 7.3E-03 for veliparib; one-sided Wilcoxon rank-sum test) and had SL interaction with PARP1 in DepMap_shRNA (P = 4.3E-03, one-side Wilcoxon rank-sum test), and *STAT3* had indirect interaction with PARP1.

2.4. Functional analysis of candidate PARPis responsive biomarkers

PARPi-related resistant or sensitive genes had the same Gene Ontology (GO) term annotations as that of PARP1/2/3 (Fig. S6), which suggests that the biomarkers have SL or SV effects with PARPis by disrupting specific molecular functions and biological processes. To explore the biological functions of candidate PARPi response biomarkers, we performed enrichment analysis using

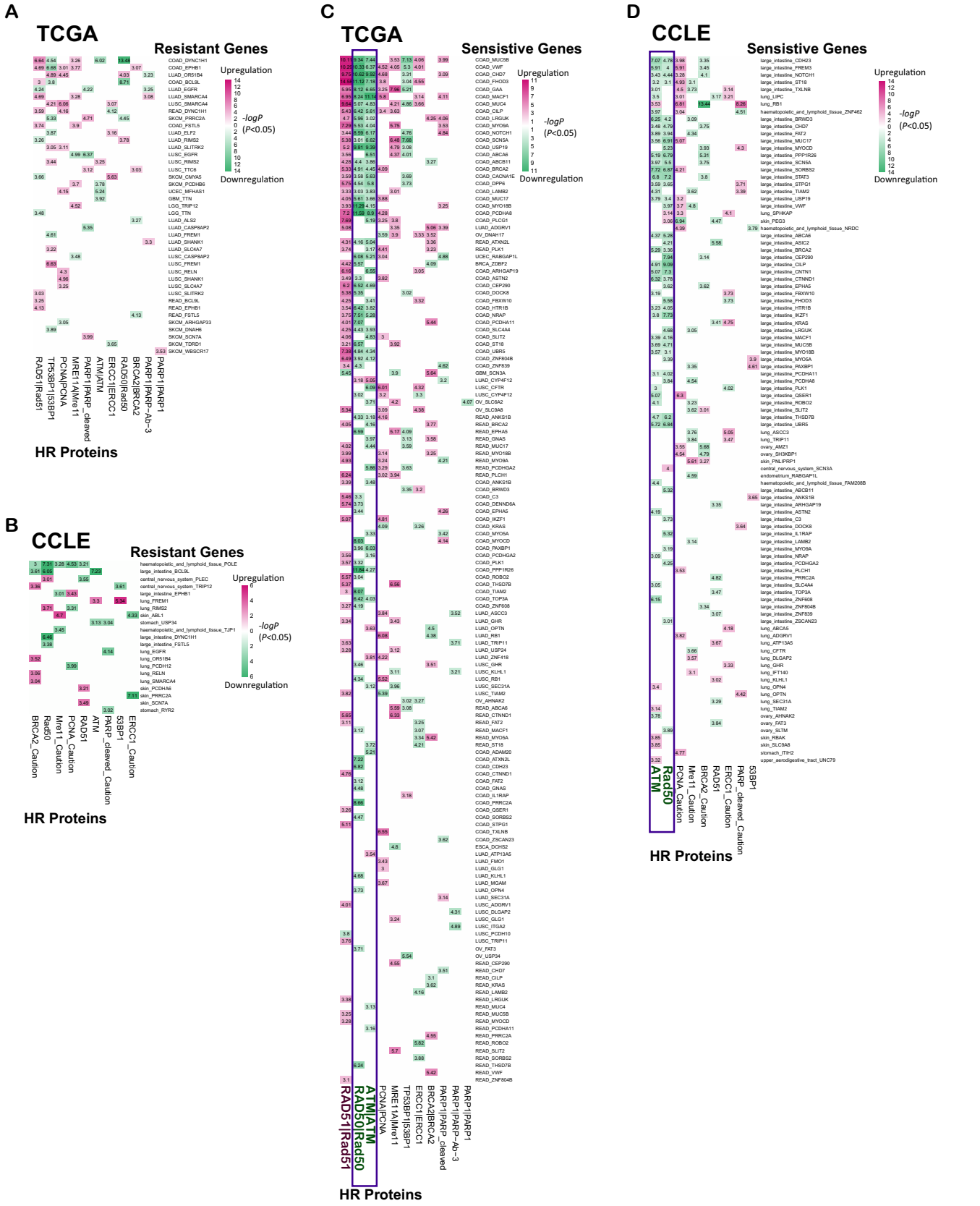

Fig. 4. Differential expression of homologous recombination (HR) proteins. (A) Resistant genes disrupt the expression of HR proteins in The Cancer Genome Atlas (TCGA). (B) Resistant genes disrupt the expression of HR proteins in Cancer Cell Line Encyclopedia (CCLE). (C) Sensitive genes disrupt the expression of HR proteins in TCGA. (D) Sensitive genes disrupt the expression of HR proteins in CCLE. Rows of the matrix indicate resistant/sensitive genes. Red entries represent upregulation of the HR proteins, and green entries represent downregulation of the HR proteins in the heatmap. Heatmap shows *-logP* values, where *P* values were calculated by one-sided Wilcoxon rank-sum test. (For interpretation of the references to color in this figure legend, the reader is referred to the web version of this article.)

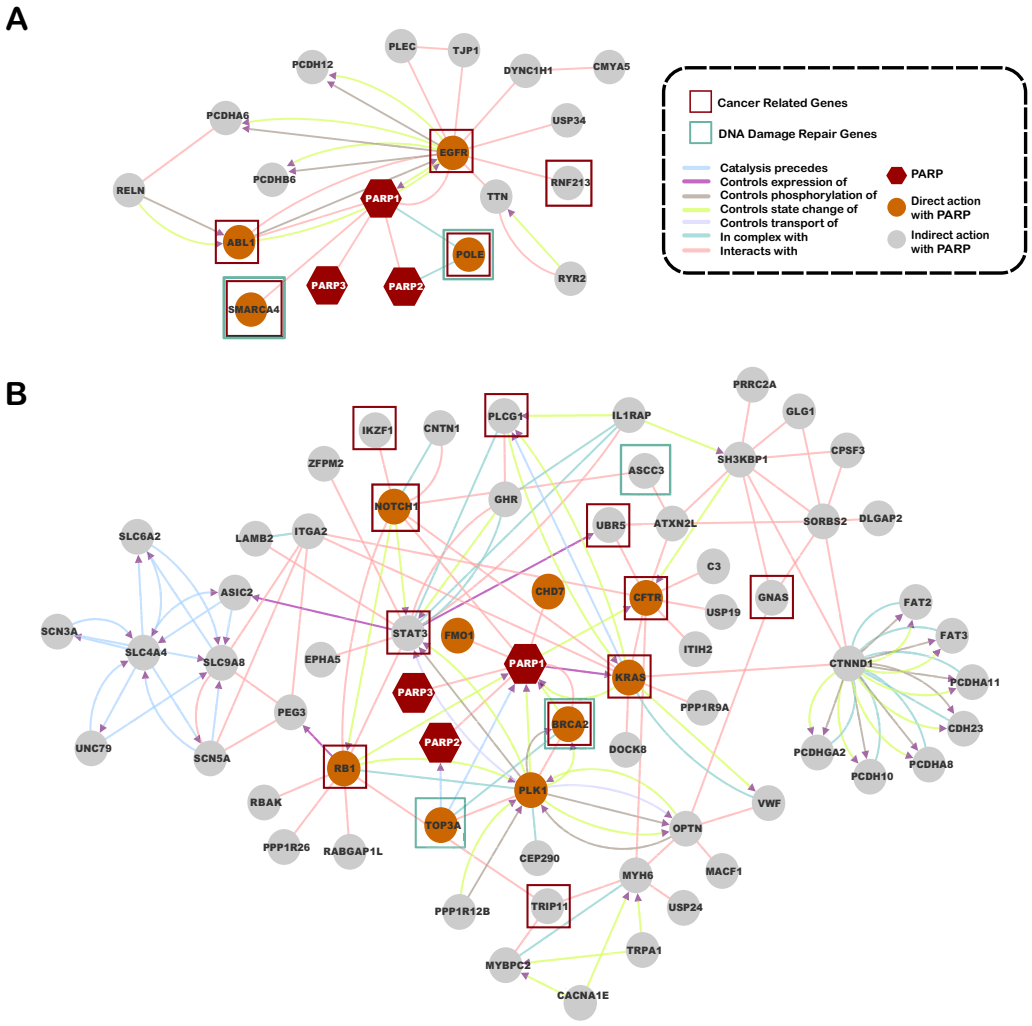

Fig. 5. Protein-protein interaction networks (PPI) between PARP1/2/3 and resistant or sensitive genes of PARP inhibitors. (A) PPI network of resistant genes and PARP1/2/3. (B) PPI network of sensitive genes and PARP1/2/3. Red nodes represent PARP1/2/3, orange nodes indicate genes that have direct interactions with PARP1/2/3, and gray nodes are genes that have indirect interactions with PARP1/2/3. Color of the edges denotes seven types of interaction relationships. Red squares represent cancer genes, and green squares represent genes with DNA damage repair function. (For interpretation of the references to color in this figure legend, the reader is referred to the web version of this article.)

molecular function and biological process terms from the GO database.

Resistant genes of PARPis were significantly enriched in molecular functions associated with microtubule and dynein activities, such as "ATP-dependent microtubule motor activity, minus-end-directed" (Fig. 6A; P = 9.28E-06, hypergeometric test), "dynein intermediate chain binding" (Fig. 6A; P = 4.08E-05, hypergeometric test), and "dynein light intermediate chain binding" (Fig. 6A; P = 4.08E-05, hypergeometric test). Paclitaxel can stabilize cellular microtubules and block chromosome segregation, and has shown success in clinical treatment of breast and ovarian cancers. Therefore, PARPi resistance can be overcome by combining it with paclitaxel. Sensitive genes of PARPis were significantly enriched in "calcium ion binding" (Fig. 6B; P = 3.97E-06; hypergeometric test), "alpha-1, 4-glucosidase activity" (Fig. 6B; P = 1.61E-04; hypergeometric test), and "maltose alpha-glucosidase activity" (Fig. 6B; P = 1.61E-04; hypergeometric test). Calcium (Ca^{2+}) signaling is involved in regulating important biological processes such as apoptosis [21]. Thus, these results indicate that mutations in sensitive genes induce an increase in free Ca^{2+}, which could promote cancer cell death.

Resistant genes of PARPis were significantly enriched in biological processes of tyrosine phosphorylation and synaptic transmission, such as "peptidyl-tyrosine phosphorylation" (Fig. 6C; P = 1.02E-05; hypergeometric test), "positive regulation of synaptic transmission, glutamatergic" (Fig. 6C; P = 1.96E-05; hypergeometric test), and "positive regulation of excitatory postsynaptic potential" (Fig. 6C; P = 2.87E-05; hypergeometric test). Tyrosine phosphorylation governs many cancer hallmarks, such as cell proliferation [22], which could induce resistance to PARPis. Sensitive genes of PARPis were significantly enriched in multiple biological processes such as "homophilic cell adhesion via plasma membrane adhesion molecules" (Fig. 6D; P = 3.69E-06; hypergeometric test), "aortic valve morphogenesis" (Fig. 6D; P = 4.91E-05; hypergeometric test), and "sodium ion transmembrane transport" (Fig. 6D; P = 1.51E-04; hypergeometric test). Adhesive interactions play a critical role in metastatic cancer dissemination [23].

2.5. Mutations in PARPi response-related gene sets to indicate prognosis

As the mutation frequency of individual PARPi response-related genes was quite low, we merged the PARPi resistant or sensitive genes in one specific cancer tissue or biological process to form a gene set. For candidate resistant genes, we focused on three genes (*TNN*, *PLEC*, and *TRIP12*) in the central nervous system cell lines,

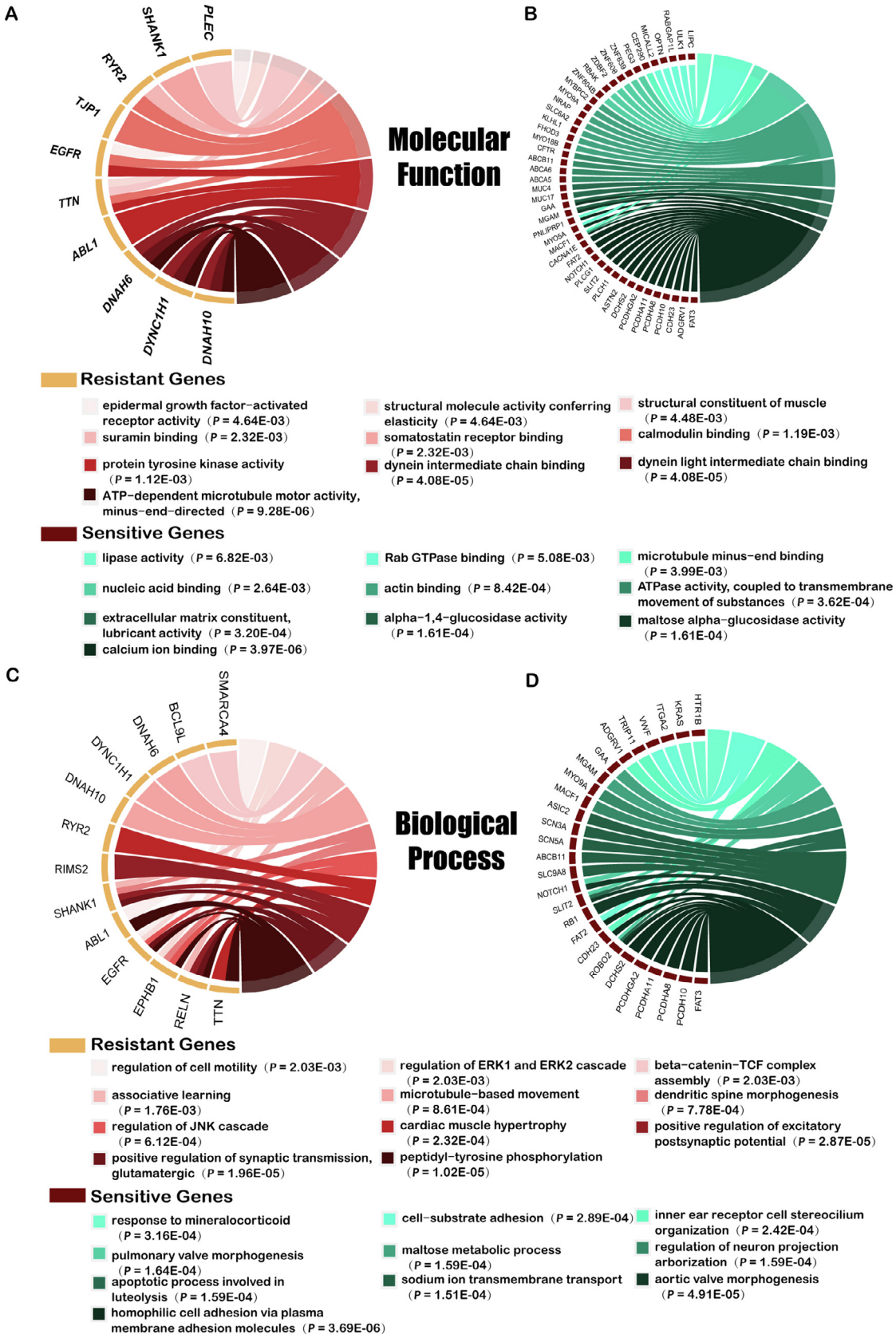

Fig. 6. Gene Ontology (GO) enrichment terms for candidate resistant and sensitive genes of PARP inhibitors. (A) Resistant and (B) sensitive gene enrichment with GO term "molecular function." (C) Resistant and (D) sensitive gene enrichment with GO term "biological process." Red and green circles indicate resistant and sensitive gene enrichment, respectively. Graph exhibits the top 10 enrichment results with false discovery rate (*FDR*) < 0.1. Left part of the circles represent resistant or sensitive genes, and right part of the circles represent the enrichment terms. (For interpretation of the references to color in this figure legend, the reader is referred to the web version of this article.)

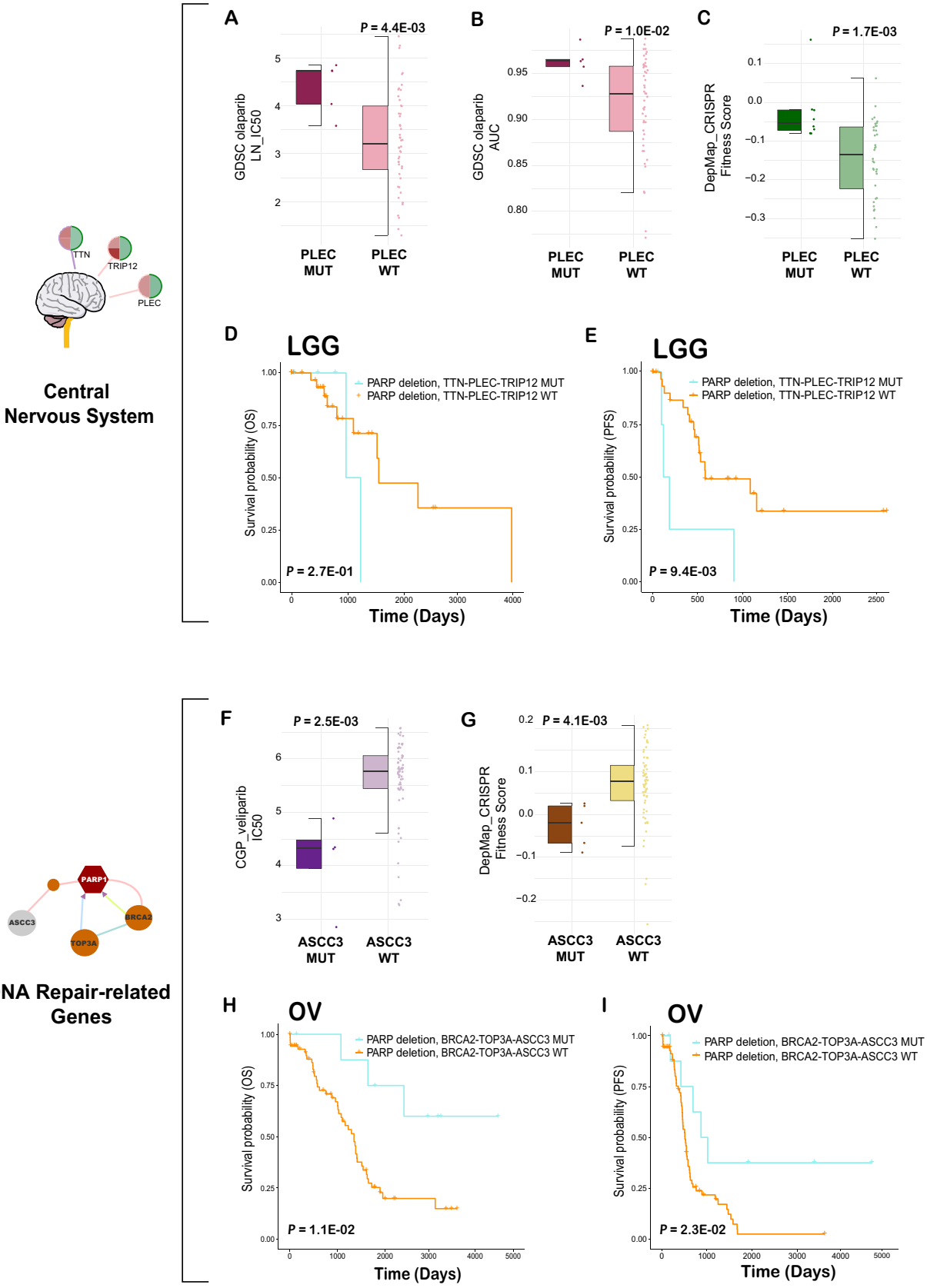

Fig. 7. PARP inhibitors response-related gene sets to indicate prognosis. (A)-(C) Central nervous system cell lines with PLEC mutation were resistant to olaparib in Genomics of Drug Sensitivity in Cancer (GDSC; LN_IC50, area under the curve [AUC]), and had better viability when PARP3 were knocked down. (D)-(E) Kaplan-Meier overall survival (OS) and progression-free survival (PFS) analysis of lower grade glioma (LGG) patients is represented in two groups: TTN, PLEC, and TRIP12 mutations, and others. (F)-(G) Lung cell lines with ASCC3 mutation were sensitive to veliparib in Cancer Genome Project (CGP; IC50), and had worse viability when PARP2 were knocked down. (H)-(I) Kaplan-Meier OS and PFS analysis of ovarian cancer patients with BRCA2, ASCC3, and TOP3A mutations, and others. P values were calculated based on log-rank test.

which were detected in lower grade glioma (LGG) and glioblastoma (GBM) from TCGA (Fig. 3Q-V and 7A-C). In LGG patients with PARP copy number deletions (as a simulation of PARP inhibition), those with mutations in the resistant gene set showed poorer prognosis than those without mutations in this gene set (Fig. 7D, E; P = 0.27; log-rank test with overall survival [OS]; P = 9.4E-03, log-rank test with Progress Free Survival [PFS]). At the transcriptome level, in cancer patients with PARP1/2/3 downregulation (also a simulation of PARP inhibition), cholangiocarcinoma (CHOL) and kidney renal papillary cell carcinoma (KIRP) patients with mutations in this candidate resistant gene set had worse PFS than those without mutations in this candidate resistant gene set (Fig. S7A, B; P = 1.9E-04, log-rank test with PFS, CHOL; P = 9.4E-03, log-rank test with PFS, KIRP).

For candidate sensitive genes, we focused on three DDR genes (*BRCA2*, *TOP3A*, and *ASCC3*), which interacted with PARP1/2/3 (Fig. 3A-C, 3K-P, and 7F, G). Ovarian cancer (OV) patients with PARP copy number deletions and mutations in the DDR gene set showed better survival than those without mutations in this gene set (Fig. 7H, I; P = 0.011, log-rank test with OS; P = 0.023, log-rank test with PFS). In OV patients with PARP1/2/3 downregulation, patients with mutations in the DDR gene set showed better prognosis than those without mutations in this gene set (Fig. S7C, D; P = 1.4E-03, log-rank test with OS; P = 0.011, log-rank test with PFS). Prognostic analysis demonstrated the reliability of our predicted candidate biomarkers for PARPis.

2.6. Prediction of drug combination for PARPis

Frequently acquired resistance to PARPis has spurred efforts to combine PARPis with other agents, such as chemotherapeutic agents, cell cycle checkpoint inhibitors, antiangiogenic agents, and PI3K inhibitors [1]. Inhibition of resistance-related activated mutations may provide clues to develop a combination strategy for PARPis (Fig. 1D). Cancer cell lines with *EGFR* mutations tended to be resistant to olaparib according to the pharmacogenomic data in CTRP (Fig. 8A; P = 6.5E-03, one-sided Wilcoxon rank-sum test), and had SV interaction with *PARP2* knockdown (Fig. 8B; P = 9.9E-03, one-sided Wilcoxon rank-sum test). Cancer patients or cell lines with *EGFR* mutations showed significantly higher expression of *EGFR* at the gene and protein levels than those without *EGFR* mutations (Fig. 8C-G; P < 0.05, one-sided Wilcoxon rank-sum test). EGFR is one of the targets of erlotinib. According to the drug combination sensitivity score (CSS) for PARPis from DrugComb data portal, the CSS of the *EGFR* inhibitor erlotinib and PARPi ABT-888 (veliparib) in human lung cancer cell line MSTO were ranked one and two (Fig. 8H).

Fig. S8 shows the drug-target and PPI networks provided by DrugComb. Many targets of erlotinib interacted with veliparib or PARP1/2, indicating the potential cross talks between erlotinib and veliparib. Cancer xenografts show that combination treatment with erlotinib and olaparib has a markedly enhanced anticancer effect in human ovarian cancer cell line A2780 [24].

In LGG patients with PARP1/2/3 copy number deletions or downregulation of expression, patients with *TTN* mutations showed worse prognosis than those with wild type *TTN* (Fig. S9A, P = 8.4E-06, log-rank test with OS; Fig. S9B, P = 1.7E-05, log-rank test with PFS). The mutation frequency of *TTN* was 48.6% (17/35) and 43.2% (19/44) in Catalog of Somatic Mutations in Cancer (COSMIC) and CCLE central nervous system cell lines, respectively, and 11.4% (58/508) and 26.1% (6/23) in LGG patients from TCGA and cBioportal, respectively. In cancers, *TTN* stimulates angiogenesis by elongation, migration, and sprouting of endothelial cells [25]. According to a phase III PAOLA-1/ENGOT-ov25 trial, the combina-

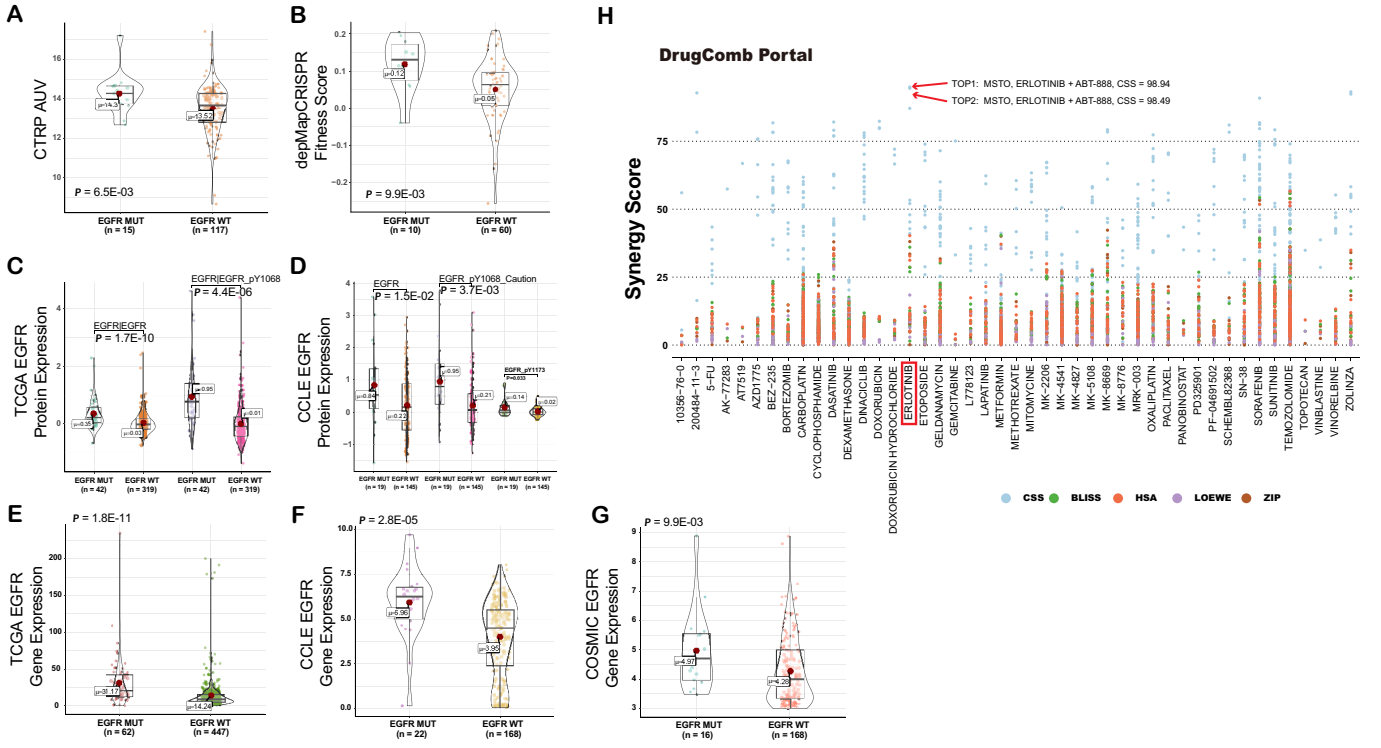

Fig. 8. Drug combination of PARP inhibitors (PARPis) and *EGFR* inhibitor. (A) Comparing area under the curve (AUC) from Cancer Therapeutics Response Portal (CTRP) and (B) fitness score (DepMap_CRISPR) in cell lines with and without *EGFR* mutation. (C)-(D) Boxplots show the distribution of EGFR protein expression (The Cancer Genome Atlas [TCGA] and Cell Line Encyclopedia [CCLE]) in cell lines with mutation of resistant gene *EGFR* and those with wild type expression (P < 0.05). (E)-(G) Boxplots show the distribution of *EGFR* expression (TCGA, Catalog of Somatic Mutations in Cancer [COSMIC], and CCLE) in cell lines with resistant gene *EGFR* mutation compared with wild type expression (P < 0.05). P values were calculated by one-sided Wilcoxon rank-sum test, and μ is the mean value. (H) Prediction of drug combination with PARPis in DrugComb Portal Database. Color of the dots represents five synergy prediction models (PLISS, HSA, LOEWE, ZIP, and CSS). The top one and two CSS are combined TBT-888 (veliparib) with erlotinib in MSTO.

tion of olaparib and bevacizumab extended PFS in patients with advanced-stage ovarian cancer, regardless of the mutation status of *BRCA1/2*. Hence, we conjectured that LGG patients with *TTN* mutations might benefit from the treatment of combining PARPis and antiangiogenic drugs, such as bevacizumab.

3. Discussion

Our study proposed a novel computational methodology to identify candidate responsive biomarkers for PARPis based on the GI network of PARP1/2/3 according to large-scale CRISPR/Cas9 and RNAi screens, and PARPi pharmacological screening data. In total, we identified 41 resistant genes and 130 sensitive genes related to PARPis. Most PARPi response-related genes were associated with HR deregulation, and interacted with PARP1/2/3 in the PPI network. Functional analysis indicated that tyrosine phosphorylation imbalance might mediate the response of PARPis in cancer cells. Furthermore, in patients with copy number deletion or downregulation of PARP 1/2/3, LGG patients with mutations in the candidate resistant gene set (*TNN*, *PLEC*, and *TRIP12*) showed poor prognosis, and OV patients with mutations in the sensitive gene set (*BRCA2*, *TOP3A*, and *ASCC3*) had better prognosis. In addition, we predicted a combination therapy of EGFR inhibitor (erlotinib) and PARPi (veliparib) in lung cancer patients, and that LGG patients with *TTN* mutation can be treated with a combination of PARPis and antiangiogenic drugs (bevacizumab). Thus, our findings provide an avenue for expanding the scale of beneficiary cancer patients for whom PARPi can be considered, and provide novel treatment options to target resistance mechanisms of PARPis.

Among the 41 resistant and 130 sensitive genes, *PRRC2A*, *USP34*, and *DNAH10* overlapped, which was not contrary to our hypothesis because mutations of these three genes mediate the response to PARPis in different cancer types. In different cancers, the gene mutation frequency is quite different. For example, *IDH1* was mutated in 77.3% (394/510) LGG samples, but showed < 12% mutation in other cancer types in TCGA. Moreover, the basic drug sensitivity of cell lines is tissue-specific. Therefore, we used our computational methodology on samples of specific cancer types and cell lines from specific tissues. However, statistical power was limited by the small sample sizes of specific cell line tissues. Thus, we did not use *FDR* to filter the biomarkers. Notably, PARPi biomarkers revealed by our method were validated in different pharmacological datasets via the HR mechanism and function correlation.

Preclinical and clinical research on combination strategies encompassing PARPis are ongoing to expand the scope of benefit in patients and overcome resistance to PARPis. Relevant clinical studies have suggested the use of a combination of PARPis and immune checkpoint inhibitors with anticancer activity in many cancer types. Combination of PARPis with bevacizumab or chemotherapy has significantly improved PFS in patients with OV [26]. In our study, we predicted combination strategies for PARPis by directly targeting PARPi resistant biomarkers such as *EGFR* and *TTN*. We estimated the functional effects of somatic mutations according to transcriptome and proteome expression data, and identified *EGFR* mutations as gain-of-function mutations. However, further detailed and in-depth analyses, such as structure analysis and animal model experiments, are warranted in future.

Cancer patients with HR defect can benefit from the use of PARPis, thereby providing new opportunities for cancer treatment modalities. We proved our hypothesis that resistant or sensitive genes could disrupt HR to mediate the response to PARPis in cancer cells. HR analysis results showed that downregulated expression of RAD50 and ATM protein expression were associated with candidate sensitive gene mutations. Moreover, we found that RAD51 expression was significantly upregulated by 51.1% (72/141) sensitive genes in TCGA. However, previous studies have indicated that upregulation of RAD51 contributes to drug resistance in cancer cells [27]. RAD51 has also been identified as a tumor suppressor, and the upregulation of RAD51 may mediate cancer cells to be sensitive to PARPis, which warrants further experiments [28].

In summary, our study systematically predicted candidate resistant and sensitive biomarkers for PARPis, pan-cancer, by constructing a cancer genome GI network. Consequently, this could pave the way for novel treatment options to target resistance mechanisms or acquired vulnerabilities of target drugs, and guide precise combination therapies.

4. Conclusion

PARPis have emerged as a beneficial therapeutic option for ovarian, breast, pancreatic, and prostate cancers. However, expanding the scale of patients who can benefit from PARPis and overcoming drug resistance are critical for furthering precision medicine. Our study systematically identified candidate responsive biomarkers (resistant and sensitive biomarkers within specific cancer tissues) for PARPis, by constructing GIs in the cancer genome. Gene mutations may mediate resistance or sensitivity to PARPis by disrupting the HR mechanism. Furthermore, by analyzing the transcriptome and proteome data, we found that *EGFR* with gain-of-function mutation induced resistance to PARPis, and predicted the combination therapy of PARPi (veliparib) and *EGFR* inhibitor (erlotinib) for lung cancer. Therefore, this study paves the way for precise combination therapies with PARPis for cancer.

5. Material and methods

5.1. Identification of PARP-related GIs

We used two publicly available CRISPR-Cas9 screening datasets. DepMap Portal (https://depmap.org/portal/) (version, 19Q1), which consists of 558 cell lines, and parental cell lines from CCLE. DepMap Portal (version, 19Q1) uses Avana CRISPR-Cas9 genome-scale knockout library and CERES algorithm to estimate gene dependency, wherein a lower CERES score indicates more essential genes [29]. Gene mutation information of cell lines was downloaded from the DepMap Portal (version, 19Q1). Another CRISPR-Cas9 fitness screen was obtained from DepMap Project Score (https://score.depmap.sanger.ac.uk/). We used the CRISPR depletion log-transformed fold change values (fitness scores) to represent the ability required for cell growth or viability, wherein a lower score indicated that a gene was more essential [30]. Gene mutation profiles of 324 cell lines were downloaded from COSMIC (https://cancer.sanger.ac.uk/cosmic).

RNAi screens were downloaded from the DepMap Portal, Achilles 2.20.2, which includes genome-scale RNAi-based loss-of-function screens of 501 cell lines [31]. We used gene knockdown viability effects (gene dependency scores) for further analysis. Here, higher shRNA scores indicated enhancement of cell viability and a gene with lower dependency score was considered more essential. However, there was no shRNA depletion scores for PARP2 in this dataset.

For somatic mutation data processing, we excluded mutations in the 5′-flanks, introns, intergenic regions, 5′-UTR, and 3′-UTR, and excluded silent mutations [32]. For cell lines with knockdown of PARP1/2/3, a one-sided Wilcoxon rank-sum test was used to test whether the fitness scores were significantly different in cell lines with and without mutation of gene A. If the fitness scores of gene A mutation samples were significantly higher or lower than that of the wild type samples ($P < 0.01$), gene A was predicted as a candi-

date partner gene with an SV or SL interaction with PARP1/2/3 (Fig. 1A).

5.2. Identification of PARPi candidate responsive biomarkers

We downloaded pharmacological screening data from GDSC (https://www.cancerrxgene.org/), CTRP, and Cancer Genome Project (CGP) (Table S2) [33]. We obtained LN_IC50 (natural log of the fitted half-maximal inhibitory concentration) values and AUC (area under the drug inhibition curve) values of five PARPis (olaparib, veliparib, talazoparib, rucaparib, and niraparib) from GDSC, two PARPis (olaparib, veliparib) from CTRP, and IC50 values of two PARPis (olaparib, veliparib) from CGP. The cell line information of the GDSC and CGP datasets was referenced from COSMIC, and cell line information of CTRP was available from CCLE.

For more than three cell lines in a specific tissue, we tested the difference in drug response values using a one-sided Wilcoxon rank-sum test between cell lines with mutated and wild type gene A. If the IC50/AUC values of cell lines with gene A mutation samples were significantly higher or lower than that of the wild type samples ($P < 0.01$), we predicted that mutations in gene A might induce resistance or sensitivity to PARPis in cancer cell lines.

5.3. Genome data from TCGA

Somatic mutation and copy number alteration (CNA) data of 32 cancer types from TCGA consortium were downloaded from Genomic Data Commons (GDC, https://portal.gdc.cancer.gov/). CNAs were determined by Genomic Identification of Significant Targets in Cancer (GISTIC2) [34]. As per Shi et al., the log2 ratio cutoff values <-0.25 were defined as deletion of PARP1/2/3 [35]. To further optimize CNAs, a one-sided *t*-test was used to select PARP1/2/3, whose copy numbers had a positive correlation with gene expression.

5.4. Survival analysis

We downloaded the OS and PFS data from TCGA. For PARP1/2/3 deficiency (deletion or downregulation), log-rank test was used to assess the difference in the survival time between patients with and without mutations of PARPi response-related genes. Kaplan-Meier plots were used to present the results (Fig. 1C). We ranked samples according to gene expression values of *PARP1*, *PARP2*, and *PARP3*. Lower quartile expression values were defined as the downregulation of PARP1/2/3.

5.5. Expression analysis

Protein expression data of CCLE cell lines were downloaded from DepMap (version 18Q4), consisting of 213 proteins across 899 cell lines. Protein expression data of 31 cancer tissues were downloaded from TCGA. All protein expression data were measured using reverse phase protein arrays. Gene expression values (transcripts per million reads) of CCLE cell lines were downloaded from the DepMap Portal (version 19Q1). Gene expression of COSMIC cell lines was log scale robust multi-array from microarray analysis. Fragments per kilobase per million mapped fragments values were used to evaluate the gene expression of TCGA samples.

We grouped samples according to the status (mutated or wild type) of PARPi response-related genes. One-sided Wilcoxon rank-sum test was used to identify the significant differential expression of HR proteins ($P < 0.05$; Fig. 1B).

To investigate the activities (gain-of-function or loss-of-function) of gene A mutation, we grouped the gene or protein expression data into two groups (gene A mutation vs. gene A wild type). Gene A mutation was considered a gain-of-function mutation if the gene or protein expression in mutated samples was significantly higher than that in the wild type samples, which was tested using the one-sided Wilcoxon rank-sum test ($P < 0.05$).

5.6. Functional analysis of PPI network

We collected 241 DNA repair-related genes from the Kyoto Encyclopedia of Genes and Genomes database, and studies by Liu et al. and Kang et al. [36–38]. There were 88 homology-dependent recombination genes. Cancer-related genes were downloaded from the Cancer Gene Census of COSMIC to explain how dysfunction of these genes drives cancer.

GO terms were downloaded from http://geneontology.org/, and a hypergeometric distribution model was used to test whether the GO terms (molecular function, biological process) were significantly enriched in the PARPis response-related genes. *P* values were corrected using the Benjamini-Hochberg correction for multiple tests, and the top 10 results with a false discovery rate (*FDR*) < 0.1 were reported (Fig. 1B).

The PPI network of PARPi response-related genes was constructed, and Cytoscape software was used to visualize the networks (https://cytoscape.org/). PPI data were assembled from the Pathway Commons database (Fig. 1B) [39].

5.7. Drug combination prediction

Drug combination prediction data were downloaded from the DrugComb Portal Database [40]. DrugComb provides drug CSS, which were interpreted as a normalized average inhibition of the drug combination response, and four other synergy prediction indexes, including bliss independence (BLISS), highest single agent (HSA), Loewe additivity (LOEWE), and zero interaction potency (ZIP). DrugComb recommends that only a drug combination that achieves a higher synergy score in all the models as well as a higher CSS should be a reliable drug combination (Fig. 1D).

We extracted the synergy prediction indexes greater than zero of PARPis, and sorted them by CSS, which involved olaparib, veliparib/AT-888, and rucaparib with 46 combination drugs from 46 cell lines. The drug-target profiles and PPI networks provided by DrugComb were obtained from PubChem (https://pubchem.ncbi.nlm.nih.gov/), ChEMBL (https://www.ebi.ac.uk/chembl/), and STITCH (http://stitch.embl.de/) databases.

Conflicts of interests

The authors declare that they have no competing interests.

CRediT authorship contribution statement

Qi Dong: Conceptualization, Methodology, Validation, Formal analysis, Investigation, Writing–original draft, Visualization. **Mingyue Liu:** Conceptualization, Methodology, Validation, Formal analysis, Investigation, Writing - original draft, Visualization. **Bo Chen:** Conceptualization, Methodology, Validation, Formal analysis, Investigation, Writing - original draft, Visualization. **Zhangxiang Zhao:** Data curation, Visualization. **Tingting Chen:** Data curation, Visualization. **Chengyu Wang:** Data curation, Visualization. **Shuping Zhuang:** Data curation, Visualization. **Yawei Li:** Methodology, Investigation. **Yuquan Wang:** Methodology, Investigation. **Liqiang Ai:** Methodology, Investigation. **Yaoyao Liu:** Methodology, Investigation. **Haihai Liang:** Writing - original draft. **Lishuang Qi:** Writing - original draft. **Yunyan Gu:** Supervision, Project administration, Writing - original draft.

Acknowledgements

The authors acknowledge the efforts of all of the researchers who have contributed the data to the public databases of COSMIC CCLE, CTRP, GDSC, GDC, TCGA, DrugComb, and DepMap. The interpretation and reporting of these data are the sole responsibility of the authors.

Author contributions

QD, MYL and BC completed data processing, analysis, and draft of the paper. ZXZ, CCT, CYW and SPZ extracted data and visualized the results. YWL, YQW, LQA and YYL provided valuable suggestions for the manuscript draft. HHL and LSQ contributed to the writing of first draft. YYG directed the study.

Funding

This work was supported by the National Natural Science Foundation of China (no. 61673143, 81872396); the Postdoctoral Scientific Research Developmental Fund (no. LBH-Q16166); the Outstanding Youth Foundation of Heilongjiang Province of China (no. YQ2021H005).

Ethics approval and consent to participate

Not applicable.

Consent for publication

The submission of this manuscript has been approved by all authors.

Appendix A. Supplementary data

Supplementary data to this article can be found online at https://doi.org/10.1016/j.csbj.2021.08.007.

References

[1] Slade D. PARP and PARG inhibitors in cancer treatment. Genes Dev 2020;34:360–94.
[2] Patel M, Nowsheen S, Maraboyina S, Xia F. The role of poly(ADP-ribose) polymerase inhibitors in the treatment of cancer and methods to overcome resistance: a review. Cell Biosci 2020;10:35.
[3] Li H, Liu ZY, Wu N, Chen YC, Cheng Q, Wang J. PARP inhibitor resistance: the underlying mechanisms and clinical implications. Mol Cancer 2020;19:107.
[4] Konstantinopoulos PA, Ceccaldi R, Shapiro GI, D'Andrea AD. Homologous recombination deficiency: exploiting the fundamental vulnerability of ovarian cancer. Cancer Discov 2015;5:1137–54.
[5] Tutuncuoglu B, Krogan NJ. Mapping genetic interactions in cancer: a road to rational combination therapies. Genome Med 2019;11:62.
[6] Wang Y, Wild AT, Turcan S, Wu WH, Sigel C, Klimstra DS, et al. Targeting therapeutic vulnerabilities with PARP inhibition and radiation in IDH-mutant gliomas and cholangiocarcinomas. Sci Adv 2020;6:eaaz3221.
[7] Gu Y, Wang R, Han Y, Zhou W, Zhao Z, Chen T, et al. A landscape of synthetic viable interactions in cancer. Brief Bioinform 2018;19:644–55.
[8] Han Y, Wang C, Dong Q, Chen T, Yang F, Liu Y, et al. Genetic interaction-based biomarkers identification for drug resistance and sensitivity in cancer cells. Mol Ther Nucleic Acids 2019;17:688–700.
[9] Shen JP, Zhao D, Sasik R, Luebeck J, Birmingham A, Bojorquez-Gomez A, et al. Combinatorial CRISPR-Cas9 screens for de novo mapping of genetic interactions. Nat Methods 2017;14:573–6.
[10] Wang T, Yu H, Hughes NW, Liu B, Kendirli A, Klein K, et al. Gene essentiality profiling reveals gene networks and synthetic lethal interactions with oncogenic ras. Cell 2017;168:890–903.e15.
[11] Horn T, Sandmann T, Fischer B, Axelsson E, Huber W, Boutros M. Mapping of signaling networks through synthetic genetic interaction analysis by RNAi. Nat Methods 2011;8:341–6.
[12] Loibl S, O'Shaughnessy J, Untch M, Sikov WM, Rugo HS, McKee MD, et al. Addition of the PARP inhibitor veliparib plus carboplatin or carboplatin alone to standard neoadjuvant chemotherapy in triple-negative breast cancer (BrighTNess): a randomised, phase 3 trial. Lancet Oncol 2018;19:497–509.
[13] Edwards SL, Brough R, Lord CJ, Natrajan R, Vatcheva R, Levine DA, et al. Resistance to therapy caused by intragenic deletion in BRCA2. Nature 2008;451:1111–5.
[14] Zhang M, Liu G, Xue F, Edwards R, Sood AK, Zhang W, et al. Copy number deletion of RAD50 as predictive marker of BRCAness and PARP inhibitor response in BRCA wild type ovarian cancer. Gynecol Oncol 2016;141:57–64.
[15] Weston VJ, Oldreive CE, Skowronska A, Oscier DG, Pratt G, Dyer MJ, et al. The PARP inhibitor olaparib induces significant killing of ATM-deficient lymphoid tumor cells in vitro and in vivo. Blood 2010;116:4578–87.
[16] Gilardini Montani M, Prodosmo A, Stagni V, Merli D, Monteonofrio L, Gatti V, et al. ATM-depletion in breast cancer cells confers sensitivity to PARP inhibition. J Exp Clin Cancer Res 2013;32:95.
[17] Telli ML, Timms KM, Reid J, Hennessy B, Mills GB, Jensen KC, et al. Homologous Recombination Deficiency (HRD) score predicts response to platinum-containing neoadjuvant chemotherapy in patients with triple-negative breast cancer. Clin Cancer Res 2016;22:3764–73.
[18] Kremerskothen J, Stölting M, Wiesner C, Korb-Pap A, Vliet V, Linder S, et al. Zona occludens proteins modulate podosome formation and function. FASEB J 2011;25:505–14.
[19] Hu H-M, Zhao X, Kaushik S, Robillard L, Barthelet A, Lin KK, et al. A quantitative chemotherapy genetic interaction map reveals factors associated with PARP inhibitor resistance. Cell Rep 2018;23:918–29.
[20] Steckel M, Molina-Arcas M, Weigelt B, Marani M, Warne PH, Kuznetsov H, et al. Determination of synthetic lethal interactions in KRAS oncogene-dependent cancer cells reveals novel therapeutic targeting strategies. Cell Res 2012;22:1227–45.
[21] Guo JLY, Chang DC. Calcium and apoptosis. Handbook of Neurochemistry and Molecular Neurobiology. Boston, MA: Springer; 2009.
[22] Hunter T. Tyrosine phosphorylation: thirty years and counting. Curr Opin Cell Biol 2009;21:140–6.
[23] Zetter BR. Adhesion molecules in tumor metastasis. Semin Cancer Biol 1993;4:219–29.
[24] Sui H, Shi C, Yan Z, Li H. Combination of erlotinib and a PARP inhibitor inhibits growth of A2780 tumor xenografts due to increased autophagy. Drug Des Devel Ther 2015;9:3183–90.
[25] Martina E, Degen M, Ruegg C, Merlo A, Lino MM, Chiquet-Ehrismann R, et al. Tenascin-W is a specific marker of glioma-associated blood vessels and stimulates angiogenesis in vitro. FASEB J 2010;24:778–87.
[26] Ray-Coquard I, Pautier P, Pignata S, Pérol D, González-Martín A, Berger R, et al. Olaparib plus bevacizumab as first-line maintenance in ovarian cancer. N Engl J Med 2019;381:2416–28.
[27] Klein HL. The consequences of Rad51 overexpression for normal and tumor cells. DNA Repair (Amst) 2008;7:686–93.
[28] Prakash R, Zhang Y, Feng W, Jasin M. Homologous recombination and human health: the roles of BRCA1, BRCA2, and associated proteins. Cold Spring Harb Perspect Biol 2015;7:a016600.
[29] Meyers RM, Bryan JG, McFarland JM, Weir BA, Sizemore AE, Xu H, et al. Computational correction of copy number effect improves specificity of CRISPR-Cas9 essentiality screens in cancer cells. Nat Genet 2017;49:1779–84.
[30] Behan FM, Iorio F, Picco G, Gonçalves E, Beaver CM, Migliardi G, et al. Prioritization of cancer therapeutic targets using CRISPR-Cas9 screens. Nature 2019;568:511–6.
[31] Tsherniak A, Vazquez F, Montgomery PG, Weir BA, Kryukov G, Cowley GS, et al. Defining a cancer dependency map. Cell 2017;170:564–576.e16.
[32] Schlafly A, Pfeiffer RM, Nagore E, Puig S, Calista D, Ghiorzo P, et al. Contribution of common genetic variants to familial aggregation of disease and implications for sequencing studies. PLoS Genet 2019;15:e1008490.
[33] Garnett MJ, Edelman EJ, Heidorn SJ, Greenman CD, Dastur A, Lau KW, et al. Systematic identification of genomic markers of drug sensitivity in cancer cells. Nature 2012;483:570–5.
[34] Mermel CH, Schumacher SE, Hill B, Meyerson ML, Beroukhim R, Getz G. GISTIC2.0 facilitates sensitive and confident localization of the targets of focal somatic copy-number alteration in human cancers. Genome Biol 2011;12:R41.
[35] Shi ZZ, Jiang YY, Hao JJ, Zhang Y, Zhang TT, Shang L, et al. Identification of putative target genes for amplification within 11q13.2 and 3q27.1 in esophageal squamous cell carcinoma. Clin Transl Oncol 2014;16:606–15.
[36] Liu C, Rohart F, Simpson PT, Khanna KK, Ragan MA, Le Cao KA. Integrating multi-omics data to dissect mechanisms of DNA repair dysregulation in breast cancer. Sci Rep 2016;6:34000.
[37] Kang J, D'Andrea AD, Kozono D. A DNA repair pathway-focused score for prediction of outcomes in ovarian cancer treated with platinum-based chemotherapy. J Natl Cancer Inst 2012;104:670–81.
[38] Kanehisa M, Furumichi M, Tanabe M, Sato Y, Morishima K. KEGG: new perspectives on genomes, pathways, diseases and drugs. Nucleic Acids Res 2017;45:D353–61.
[39] Cerami EG, Gross BE, Demir E, Rodchenkov I, Babur O, Anwar N, et al. Pathway commons, a web resource for biological pathway data. Nucleic Acids Res 2011;39:D685–90.
[40] Zagidullin B, Aldahdooh J, Zheng S, Wang W, Wang Y, Saad J, et al. DrugComb: an integrative cancer drug combination data portal. Nucleic Acids Res 2019;47:W43–51.